

Water-soluble amino derivatives of free-base dppz – syntheses and DNA binding studies†

Tim Phillips, Itshamul Haq and Jim A. Thomas*

Received 12th October 2010, Accepted 17th February 2011

DOI: 10.1039/c0ob00869a

The syntheses of two water soluble dipyrido-[3,2-*a*:2',3'-*c*]-phenazine analogues containing one or two appended amino/amide chains are reported. Steady state optical studies on the two new compounds reveal high-energy dppz-based luminescence in water and non-aqueous solvents. Optical titrations with duplex DNA show that the luminescence is quenched on the addition of DNA. Binding curves constructed from absorption and emission changes indicate that, while one of the compounds display negligible binding properties, the other binds DNA with relatively high affinity ($>10^5 \text{ M}^{-1}$). Isothermal calorimetry experiments, designed to investigate the higher binding compound in more detail, reveals that its interaction with CT-DNA is actually biphasic with one tight ($>10^5 \text{ M}^{-1}$) and one weaker binding site ($\sim 10^5 \text{ M}^{-1}$). In both cases binding is entropically driven. Further calorimetry studies involving the interaction of the new compound with a variety of polynucleotides were carried out. To aid comparisons, similar experiments involving a previously reported bipyridyldiylum derivative of dppz were also carried out. These studies reveal that the bipyridyldiylum derivative binds all these sequences monophasically with relatively low affinities ($\sim 10^4 \text{ M}^{-1}$). However, while the amino/amide chain appended derivative binds to Poly(dA).poly(dT) monophasically with relatively low affinities, it binds all the other polynucleotide studied biphasically, with affinities ranging from $<10^6 \text{ M}^{-1}$ to $>10^8 \text{ M}^{-1}$. The ITC data reveals that for both compounds thermodynamic signatures for binding are dependent on the sequence being bound. In both cases, the data for Poly(dA).poly(dT) is particularly anomalous. An analysis of the data shows that binding is selective, with affinities at flexible sequences being several orders of magnitude higher than those at more rigid sequences.

Introduction

Metal complexes designed to bind with high affinity to DNA often contain the known DNA intercalating ligand dipyrido-[3,2-*a*:2',3'-*c*]-phenazine, dppz.¹ This ligand is particularly attractive for such studies as its complexes with kinetically inert d^6 metal ions, such as Ru^{II} , Re^{I} , and Os^{II} , frequently function as DNA light-switches;² ³MLCT-based luminescence, suppressed in water due to hydrogen bonding interactions involving the phenazine unit of the dppz, is “switched on” by intercalative binding to DNA.³ With the aim of creating photo-reagents for the study of DNA or photo-activated chemotherapeutics, electron deficient metal centers⁴ and dppz-analogues⁵ have also been used to create derivatives that can photo-oxidize G-sites of DNA.

Recently, as part of our research into novel luminescent DNA binding probes,⁶ we reported on the photophysical and DNA

binding properties of entirely organic bipyridyldiylum derivatives of dppz, such as **1**, in which the bidentate N-donor coordination site of the ligand is alkylated (Fig. 1).⁷ We found that these cations can bind to DNA with affinities comparable to those of dppz based metal complexes and that the luminescence of these cations – due to a phenazine \rightarrow bipyridyldiylum intramolecular charge transfer, ICT, state – is quenched on binding to DNA, presumably by photo-oxidation of nucleobases

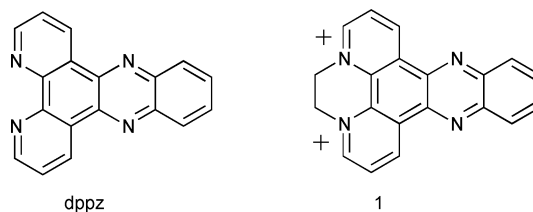


Fig. 1 Structures of dppz and compound **1**.

The photochemistry of uncoordinated free base dppz has also been explored. Work by McGovern, *et al.* has shown that this molecule has potential as a strong photo-oxidizing agent: ethanol solutions of dppz can undergo two-electron photoreduction yielding 9,14-dihydrodipyridophenazine.⁸ Given these redox properties

Dept. of Chemistry, University of Sheffield, Brook Hill, Sheffield, UK, S3 7HF. E-mail: james.thomas@sheffield.ac.uk; Fax: 44 114 222 9346

† Electronic supplementary information (ESI) available: T_m curves for CT-DNA in the presence of **2** and **3**. Typical ITC data for the interaction of **2** injected into CT-DNA. Typical ITC data for the interaction of **1** (0.75 mM) injected into poly(dG-dC)-poly(dG-dC) (0.12 mM). Synthesis of compounds **2** and **3**. See DOI: 10.1039/c0ob00869a

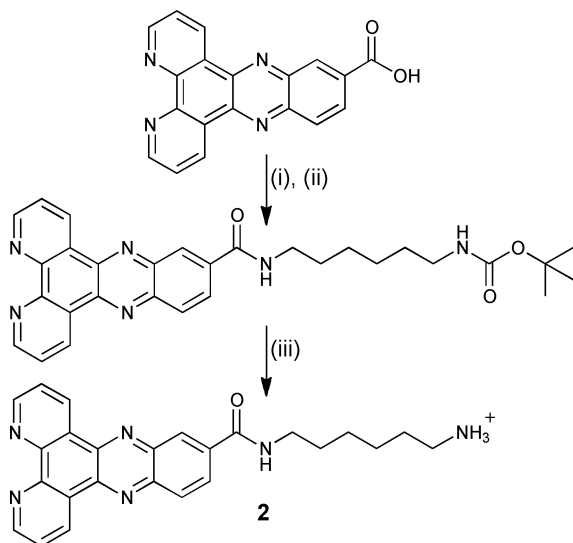
and the DNA binding properties of metal and organic dppz cations, we were interested in extending our studies on organic based systems by investigating the interaction of free base dppz-based systems with DNA. However, since dppz itself is insoluble in water, we sought methods to solubilize the free base itself.

Naturally occurring amines, such as spermine and spermidine, are polycations under *in vivo* conditions and bind to DNA with relatively high affinity. There is also some evidence that they display binding preference for A·T rich minor grooves⁹ or G·C rich major grooves.¹⁰ In several synthetic studies, amines have been tethered to a range of small molecule DNA substrates to enhance or modulate solubility and binding properties.^{11–14} Consequently, with the aim of producing water soluble systems, we set out to functionalize dppz with amino/amide chains and determine the DNA binding properties of these hybrid molecules. We also examined whether the amine chain attachment position on the dppz intercalative platform had an effect on the binding properties. Herein we describe the synthesis of, and DNA binding studies on prototype water-soluble amino derivatives of dppz.

Results and discussion

In studies into the photochemistry of DNA duplexes,^{15,16} Ossipov, *et al.* reported dppz derivatives covalently linked to DNA. In this study they used dipyridylphenazine-11-carboxylic acid to construct glycerol phosphoramidites-appended oligonucleotides.¹⁵ It occurred to us that the alkylamide tethered dppz intermediate prepared in these studies could form the basis of possible DNA binding substrates in themselves.

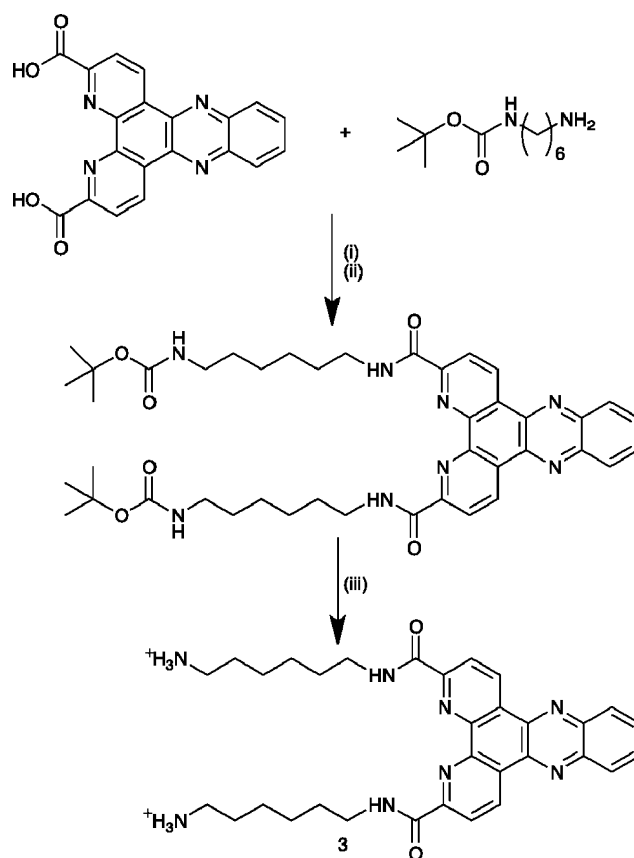
Using their methods, we synthesized the monocation *N*-(6-aminohexyl)dipyridophenazine-amide, **2** (Scheme 1). As reported by Ossipov, *et al.*, we found that the required amide derivative of dipyridophenazine-2-carboxylic acid could only be synthesized if the carboxylic acid was first treated with 1,1'-carbonylbis[1*H*-imidazole] in dry pyridine. Immediate addition of the protected amine to this mixture gave the corresponding amide in acceptable yields. Removal of the Boc protecting groups with anhydrous tri-



Scheme 1 Synthesis of compound **2**. (i) 1,1'-carbonylbis[1*H*-imidazole] in dry pyridine (ii) *N*-Boc-1,6-diaminohexane (iii) Anhydrous trifluoroacetic acid (TFA) in dichloromethane.

fluoroacetic acid, TFA, in dichloromethane afforded the product as its trifluoroacetate salt. Compound **2** is soluble in a range of solvents including methanol and water.

To investigate whether DNA binding is affected by the number and positioning of the amine chains tethered to the dppz unit, we reacted the same Boc protected amine with the previously reported 3,6-dicarboxylic acid derivative of dppz¹⁷ using a procedure adapted from Perrée-Fauvet *et al.*¹⁸ (Scheme 2). Again, deprotection of the *N*-terminal Boc protecting groups with a 1 : 1 mixture of anhydrous TFA in dichloromethane afforded the product, compound **2**, in reasonable yield as the trifluoroacetate salt. This dication shows good solubility in methanol but, somewhat surprisingly, it is less water-soluble than the monocation **1**.



Scheme 2 Synthesis of compound **3**. (i) *N*-Boc-1,6-diaminohexane in anhydrous DMF (ii) BOP/diisopropylethylamine/5% aqueous NaHCO₃ (iv) Anhydrous trifluoroacetic acid (TFA) in dichloromethane.

Optical spectroscopy studies

The UV-visible absorption spectra of **2** and **3**, recorded in methanol are very similar to that of dppz. Between 215 and 385 nm, they display a series of intense $\pi \rightarrow \pi^*$ bands (Table 1).

Steady state photoexcitation of methanol solutions of **2** and **3**, with a range of wavelengths between 280 and 415 nm, results in a broad emission centered at 523 and 512 nm, respectively. Again, this is very similar to the $\pi \rightarrow \pi^*$ based emission observed for dppz, which is seen as a broad band with a maximum at 544 nm in ethanol.¹⁹ Furthermore, analysis of excitation spectra showed that the emission is from the expected compound and not an

Table 1 Summary of the absorption and emission data for compounds **2** and **3**

Compound	Absorption ^a λ_{\max} (nm) (ϵ (M ⁻¹ cm ⁻¹))	Emission ^b (nm)
2	209 (21000), 242(sh), 272 (36900), 295 (sh), 363 (8800), 382 (9400)	523 (methanol) 445 (water)
3	215 (35900), 237 (27000), 278 (45100), 306 (sh), 363 (13700), 382 (13000)	512 (methanol) 535 (water)

^a in methanol. ^b $\lambda_{\text{ex}} = 350$ nm.

impurity. Interestingly, while the emission λ_{\max} for **3** shows some sensitivity to changes in solvent (with a red shift of $\Delta\lambda_{\text{em}} = 23$ nm in water), the energy of emission for **2** displays appreciable blue shifting in water, where $\lambda_{\max} = 445$ nm. This suggests that either the energy of HOMO for the $\pi \rightarrow \pi^*$ based emission has been lowered, or its LUMO energy is raised. The biggest structural difference between **2** and **3** is that the alkylamide group is attached to the phenazine unit of **2**, while for **3** attachment is at the dipyrindyl moiety. Furthermore, DFT calculations on free-base dppz have indicated that HOMO for its lowest energy transition is centered on the phenazine moiety, while LUMO is on the dipyrindyl unit.⁸ Thus, solvent dependence for the emission energy for **2** may be the result of the alkylamine unit of compound hydrogen bonding with water and so lowering HOMO involved in the emission. The red shift in the emission of **3** in water is consistent with increased hydrogen bonding in this solvent, as such an interaction would lower LUMO of the same transition. The difference in magnitude of this effect for the two compounds may reflect the accessibility of the amino groups towards hydrogen bonding.

DNA binding studies

Optical titrations

The interaction of the two new compounds with calf-thymus DNA, (CT-DNA), was initially investigated. While **2** was sufficiently soluble for these studies to be carried out in simple aqueous buffer solutions, studies on **3** required buffer solutions made up in 95 : 5 v/v water/DMSO mixtures. This solvent mixture is commonly used in such studies,²⁰ furthermore UV and circular dichroism experiments, as well as T_m studies within this lab have shown that neither the structure nor stability of duplex DNA is affected by these conditions.

The ΔT_m of CT-DNA with **2** and **3** were studied at approximately 50% of binding sites saturation, see ESI†. In the conditions employed CT-DNA displayed a T_m of 73 °C. DNA melting curves in the presence of **2** show that, even at temperatures as high as 95 °C, the duplex is not completely denatured; therefore ΔT_m cannot be accurately determined, although we estimate that the stabilization is between 8–10 °C. In contrast, in the same conditions, ΔT_m for **3** is only around 1 °C, indicating that the interaction of this compound with CT-DNA is considerably weaker than that for **2**.

To assess the DNA binding parameters of both new compounds in more detail absorption titrations using CT-DNA were carried out. Addition of DNA to buffered aqueous solutions of compound **2** results in distinctive large hypochromicities in all its absorption bands; for example, the low energy band between 320 and 400 nm shows up to 62% maximum hypochromicity (Fig. 2A).

When analyzed these data produced classical saturation binding curves (Fig. 2B). Using the changes of absorption at 370 nm, data

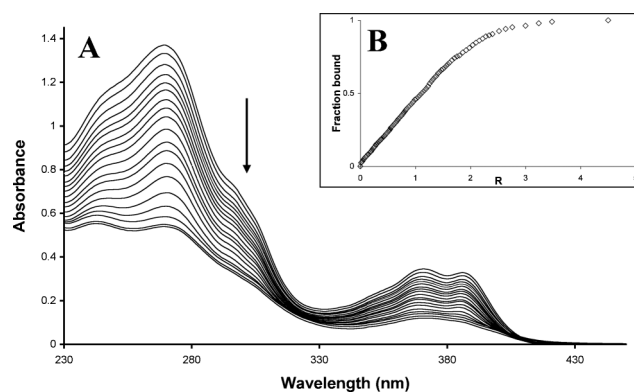


Fig. 2 (A) Typical UV-visible titration for **2** with CT-DNA. (conditions: $[2] = 40 \mu\text{M}$, 25 °C, 5 mM Tris buffer, 25 mM NaCl, pH 7.0, 1 cm pathlength). (B) Binding curve constructed from this raw data.

fits to the McGhee–von Hippel model for non-cooperative binding to an isotropic lattice,²¹ resulted in estimates for the equilibrium binding constant of $K_b = 7.40 \times 10^5 \text{ M}^{-1}$ and a site size, S , of 1.95 bp, a value that is slightly higher than that obtained in similar experiments on $[1](\text{NO}_3)_2$ (2.22×10^5).^{7a} In contrast, although the equivalent low energy band of **3** initially displayed some minimal hypochromicity, after the first two or three titers of CT-DNA very little DNA induced change was observed in the absorption spectrum for this compound.

It was found that the luminescence of the compounds was modulated by DNA binding. For compound **2**, addition of CT-DNA resulted in appreciable *reduction* in steady state luminescence intensity accompanied by a band red-shift of 8 nm (Fig. 3); similar effects have previously been observed. While the emission from compound **1** was completely quenched at high $[\text{DNA}]:[1]$ binding ratios due to photo-oxidation by both G and A sites, other derivatives displayed behavior similar to that observed for

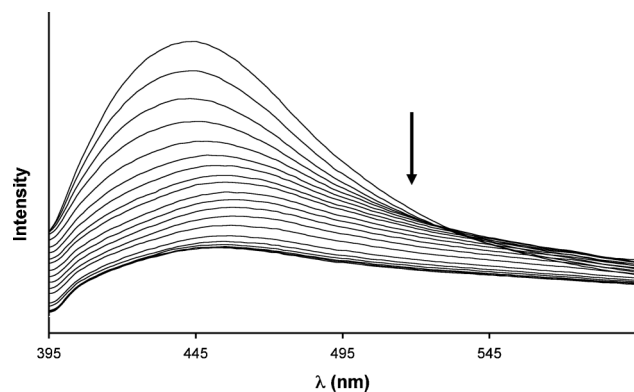


Fig. 3 Luminescence titration for **2** with CT-DNA. (conditions: $[2] = 40 \mu\text{M}$, 25 °C, 5 mM Tris buffer, 25 mM NaCl, pH 7.0, $\lambda_{\text{ex}} = 350$ nm.).

2 and this was interpreted as being due to a combination of two processes involving intercalated substrates: quenching at redox active G-steps, and blue shifted emission at non-G sites.^{7b}

Again these luminescent changes produced typical binding curves which, when fitted to the McGhee–von Hippel model, yielded a second estimate for binding parameters, with $K_b = 1.8 \times 10^5 \text{ M}^{-1}$ and $S = 1.58 \text{ bp}$, which are comparable to the value obtained from the absorption titration data and very close to that obtained for **[1](NO₃)₂**. Again, when corresponding experiments were carried out on complex **3**, although some minimal reduction in luminescence was observed, it was too small to produce reliable binding curves. Given these results, and those obtained from the absorption studies, it seems that **3** binds to duplex DNA with, at best, a low binding affinity; whereas, the binding parameters obtained for **2** are comparable to those of **1**. We explored the nature of this latter interaction in more detail through viscosity, which offers a simple method to distinguish DNA binding mode with authority.

While classical groove binders do not affect the viscosity of DNA solutions, intercalation results in a lengthening and stiffening of DNA producing a concomitant increase in the relative specific viscosity of aqueous DNA solutions.²²

We found that in contrast to effect of the known groove binder²³ H33258, which produces no overall change in the viscosity of DNA solutions, the addition of **2** results in increases in the relative specific viscosity of CT-DNA solutions, Fig. 4, confirming that **2** intercalates into DNA. However, unlike **1**, compound **2** has potential to recognize DNA through additional groove binding interactions involving its alkyl amine moiety. Further details on the nature of the interaction of **2** with DNA and the thermodynamics of the binding processes are revealed through isothermal titration calorimetry (ITC) binding experiments.²⁴

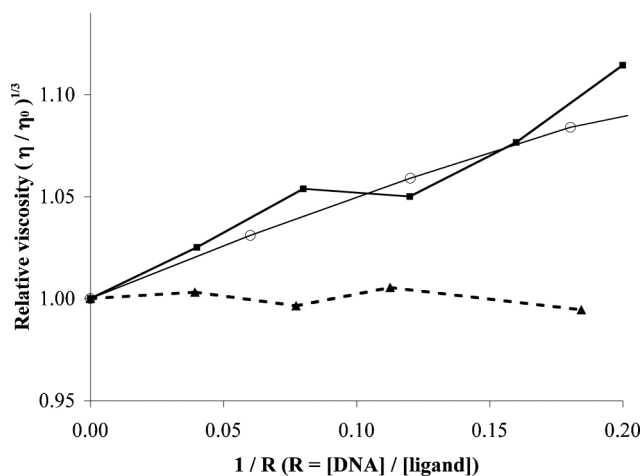


Fig. 4 Relative viscosity of CT-DNA upon addition of H33258 (▲), **1** (○) and **2**. (■) Conditions: 27 °C, 5 mM Tris buffer, 25 mM NaCl, pH 7.0).

Calorimetry studies. Repeated ITC titrations of **3** with CT-DNA only showed heat changes due to dilution of the complex at 25 °C. Titrations were repeated at different concentrations of complex and/or CT-DNA and temperature, but again no changes were observed. This lack of ITC signal indicates, at the concentrations that **3** is soluble, binding is either weak or

associated with near zero enthalpy and heat capacity change. Indeed it has been noted that ITC is not a reliable technique for interactions where $K_b < 10^4 \text{ M}^{-1}$.^{24b} These ITC observations, in conjunction with spectroscopic data reported above, offer further proof that **3** binds to CT-DNA with very low or negligible affinity. It seems that the positioning of the tethered alkylamine chains leads to unfavorable steric interactions preventing anything other than weak electrostatic binding.

However, studies on compound **2** displayed clear evidence for DNA binding. Titration plots obtained for **2** (ESI†) reveal that its interaction with CT-DNA is clearly biphasic and is best fit to a two-site model – fitting to more sites – yields a statistically worse fit. This observation is in contrast with previously reported ITC studies on **1** which revealed monophasic binding. Reversible binding of low molecular weight synthetic compounds to natural DNA sequences is often complex with ITC revealing multiple binding modes. This is simply a reflection of the heterogeneity in potential binding sites found in naturally occurring DNA sequences.

The ITC data for CT-DNA (Table 2) show that upon addition of **2** there is an initial relatively tight, entropically driven, binding event with a $K_{\text{obs}} = 4 \times 10^6 \text{ M}(\text{bp})^{-1}$. Upon saturation of these sites there is a subsequent binding mode, again entropically driven, but with lower affinity $K_{\text{obs}} = 1.4 \times 10^5 \text{ M}(\text{bp})^{-1}$. However, both of these figures are appreciably larger than the figure obtained from ITC studies on **1** ($K_b < 10^5 \text{ M}^{-1}$).

Optical binding experiments are unable to detect such subtleties in ligand–DNA interactions, and the binding parameters derived from absorption and luminescence experiments probably represent an averaged binding constant for both binding events. However, it is notable that the ITC measured parameters for one of the binding modes ($K_b = 1.4 \times 10^5 \text{ M}^{-1}$ and $S = 1.6 \text{ bp}$) are very similar to the data obtained from the absorption and luminescent titration, while the other mode displays an affinity that is over 28 times larger ($K_b = 4.0 \times 10^6 \text{ M}^{-1}$ and $S = 2.1 \text{ bp}$). Nevertheless, site sizes and affinities for both modes are comparable to data obtained for similar organic and metallo-intercalators. The thermodynamic signatures of the two modes, Table 2, are also somewhat similar, with positive enthalpic and entropic terms indicating entropically driven binding. This indicates that increases in unfavorable steric interactions outbalance enthalpically favorable stacking interactions, but are compensated by more extensive, entropically favorable, solvent/counter ion release.^{7a,25}

This is slightly different from data obtained for **1** which displays both favorable enthalpic *and* entropic terms, suggesting that the interaction between **2** and CT-DNA is largely driven by solvated water and counter-ion release.

The differences in thermodynamic signatures of DNA binding between **1** and **2** are clearly due to the presence of the additional functional groups attached to the dppz moiety in the latter compounds. For **2** and the metallo-intercalating complex

Table 2 ITC derived binding parameters and thermodynamic data for the two observed interactions of **2** with CT-DNA

N Ligand/bp	$K_{\text{obs}} (\text{M}^{-1})$	$\Delta G (\text{kJ mol}^{-1})$	$\Delta H (\text{kJ mol}^{-1})$	$T\Delta S \text{ kJ mol}^{-1} \text{ K}^{-1}$
1.6	4.0×10^6	-37.7	+6.3	+44.0
1.5	1.4×10^5	-29.4	+1.2	+30.6

[Ru(phen)₂(dppz)]³⁺ non-intercalative moieties can rest in grooves, displacing bound water from both DNA and the ligand and thus generate favourable entropic contributions to binding.²⁵ Indeed, large positive entropies are generally associated with DNA binding events involving naturally occurring polyamines such as spermine. This factor is absent from **1** where binding is entirely driven by enthalpically favourable stacking interactions and entropically favourable polyelectrolyte effects much like classical, simple intercalators such as ethidium and propidium bromide.²⁶

To further probe DNA binding thermodynamics and to remove the complicating presence of heterogeneous binding sites found in natural DNA sequences we went on to examine the binding of **2** with a series of synthetic AT and GC polynucleotides. These studies are of interest for a second reason: it is known that the structure and properties of specific duplex sequences can differ radically from that of typical genomic B-DNA. For example, it is well established that rigid A-tracks, which are associated with duplex bending, are compressed in the minor groove and widened in the major groove compared to B-DNA,²⁷ while extended G-tracks take up an A-DNA-like structures, where the major groove is narrow and deep and the minor groove is widened.²⁸ Contrastingly, a range of studies on alternating purine–pyrimidine steps indicates that they display anomalous structural flexibility;²⁹ properties that are exemplified by the TATA box sequence.³⁰ As a consequence, binding substrates can interact with these sequences in a very different manner to that observed for canonical B-DNA. To put the studies on **2** into context, the interaction of **1** with the same polymers were first investigated.

It was found that compound **1** binds to all four polynucleotides monophasically, see ESI† for a typical example. The thermodynamic data derived from titrations with all four sequences are summarized in Table 3. To aid comparisons the previously reported data for CT-DNA is also included.

The most striking observation is that, while the thermodynamic signature and binding affinities to three of the polynucleotides are comparable to those reported for CT-DNA, with favorable entropic and enthalpic terms, the parameters for binding to Poly(dA)poly(dT) are distinctly different. In the latter case, although the overall binding affinity is similar to those observed for the other polynucleotides, binding is now entirely driven by a large entropic term, with the enthalpy changes actually opposing the interaction *vide infra*.

Similar studies involving **2** reveal that the binding thermodynamics for this compound are very different. Initially, the most striking difference between the compounds is that, while **1** displays monophasic binding to all the sequences studied, **2** displays biphasic binding to all of the sequences except poly(dA-dT).poly(dA-dT); however, a closer analysis reveals further differences.

As with its interaction with CT-DNA, binding of **2** to poly(dA-dT).poly(dA-dT) is in two phases, which are mainly driven by favorable entropy changes (Fig. 5); although there is also a favorable enthalpy change, but this is smaller than that observed for the interaction of **1** with poly(dA-dT).poly(dA-dT). In contrast, both entropic terms observed for **2** are much larger than the equivalent figure for **1** (Table 4).

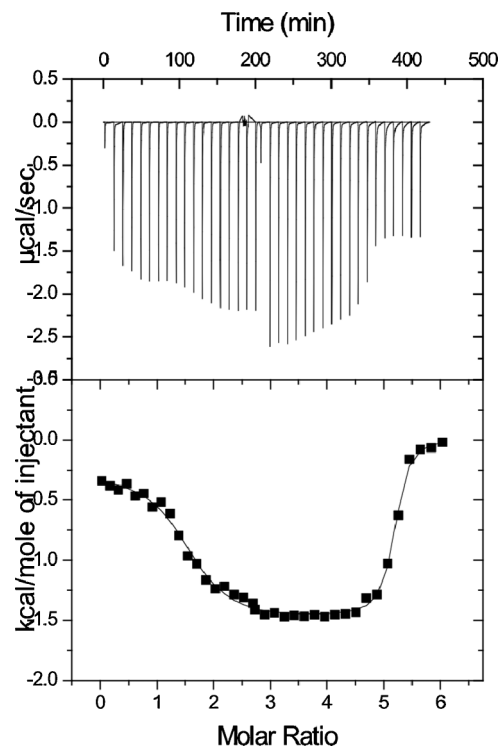


Fig. 5 Typical ITC data for the interaction of **2** (1.37 mM) injected into poly(dA-dT).poly(dA-dT) (0.1 mM) in 5 mM Tris, 25mM NaCl, pH 7.0 at 25 °C.

Consequently, the first binding affinity of **2** to this alternating polymer is more than three orders of magnitude larger than that for **1**. For the second binding mode of **2**, this difference in affinity is appreciably less ($\Delta K_{\text{obs}} \approx 50$), largely due to a decrease in the favorable entropy term.

Thermodynamic parameters for poly(dG-dC).poly(dG-dC) and poly(dG).poly(dC), are quite similar to those for poly(dA-dT).poly(dA-dT). binding affinities are higher than those observed for single phase binding of **1** and again, this effect is due to more favorable entropy changes (Table 4).

As for **1**, titrations involving **2** and poly(dA).poly(dT) are anomalous (Fig. 6). A single binding phase is observed and its

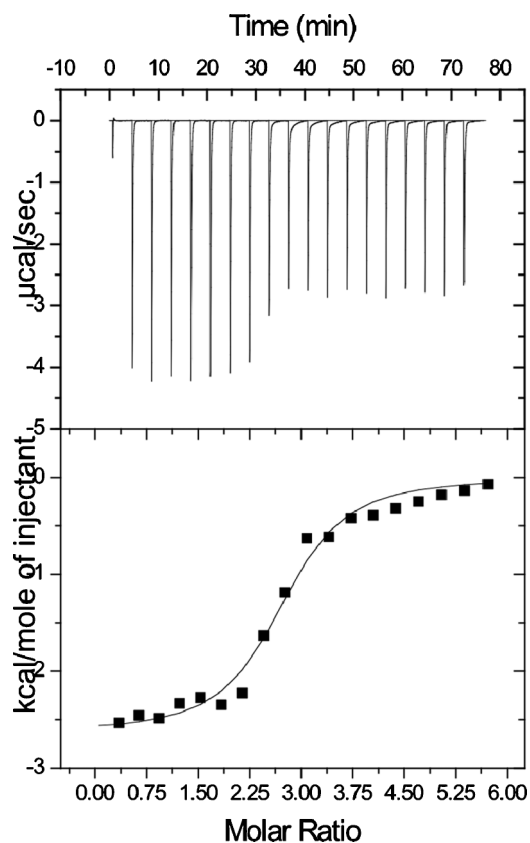
Table 3 ITC derived binding parameters and thermodynamic data for the interaction of **1** with synthetic oligonucleotides

	N Ligand/bp	K_{obs} (M^{-1})	ΔG (kJ mol^{-1})	ΔH (kJ mol^{-1})	$T\Delta S$ $\text{kJ mol}^{-1} \text{K}^{-1}$
CT-DNA ^a	3.5	5.4×10^4	-30.0	-10.9	+20.1
poly-(AT) ₂	1.5	6.4×10^4	-27.4	-8.8	+18.6
poly-(GC) ₂	1.5	3.6×10^4	-26.0	-10.9	+15.1
Poly(dG)poly(dC)	3.0	6.1×10^4	-27.3	-10.0	+17.3
Poly(dA)poly(dT)	1.6	7.4×10^4	-27.8	+16.3	+44.1

^a Data previously reported in reference 7a.

Table 4 ITC derived binding parameters and thermodynamic data for the interaction of **2** with polynucleotides

	N Ligand/bp	K_{obs} (M^{-1})	ΔG (kJ mol^{-1})	ΔH (kJ mol^{-1})	$T\Delta S$ $\text{kJ mol}^{-1} \text{K}^{-1}$
poly-(AT) ₂	1.5	1.1×10^8	-45.9	-1.1	+44.8
	3.6	3.1×10^6	-37.0	-6.4	+30.6
poly-(GC) ₂	1.3	4.9×10^7	-43.9	-3.5	+40.4
	3.6	2.6×10^6	-36.6	-6.7	+29.9
Poly(dG)poly(dC)	1.4	6.7×10^7	-44.7	-9.6	+35.1
	1.4	8.8×10^5	-34.0	-7.5	+29.9
Poly(dA)poly(dT)	2.7	2.1×10^5	-30.4	-11.0	+19.4

**Fig. 6** Typical ITC data for the interaction of **2** (1.64 mM) injected into poly(dA)poly(dT) (0.06 mM) in 5 mM Tris, 25mM NaCl, pH 7.0 at 25 °C.

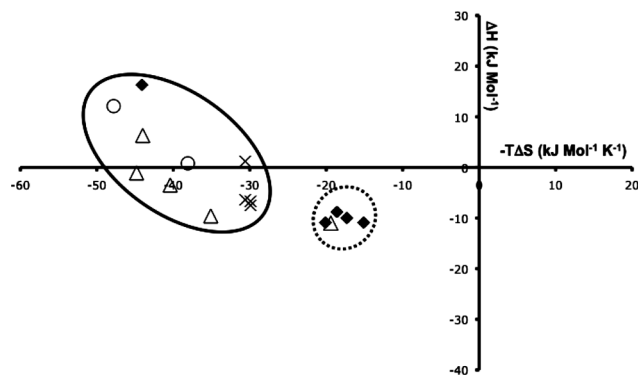
thermodynamic profile is very different to the interaction of **2** with the other sequences studied. While binding of **1** to this non-alternating sequence is due to favorable entropic changes, binding of **2** is entropically and enthalpically driven.

Although it is difficult to fully assign specific molecular details for different binding events through bulk thermodynamic parameters, it is noteworthy that the thermodynamic profile for the first binding events of **2** with the two GC polynucleotides and the alternating AT polynucleotides are very similar and hence likely to correspond to an analogous binding mode, which is very different to that observed for binding to Poly(dA)poly(dT). Furthermore, a comparison of calorimetry derived affinities reveals that, although **2** binds to both GC rich sequences with similar affinities, binding to AT steps is noticeably sequence dependent, with the alternating poly-(AT)₂ being bound over 500 times higher than the Poly(dA)poly(dT) duplex. These observations are consistent with compound **2** displaying a binding preference to flexible sequences:

as outlined above, alternating AT tracks are particularly flexible, while extended A-tracks are known to be rigid.

A similar comparison of the thermodynamic signatures for the second binding mode of **2**, again shows similarities between both GC-based sequences and the alternating AT-based polymer; however, in this case calorimetry derived affinities are considerably smaller.

Even more striking differences in affinities are apparent when a comparison between the data for **1** and **2** is made, for example, for **2** the high-affinity binding phase to poly-(AT)₂ is well over three orders of magnitude higher than the single binding phase of **1** with the same sequence. To analyze the thermodynamic differences between the binding modes of **1** and **2** in more detail entropy–enthalpy compensation plots for all the binding events involving CT-DNA and the polynucleotides were constructed (Fig. 7). To facilitate a comparison with dppz-based metal complexes the previously reported calorimetry data for the interaction of Λ - and Δ -[Ru(phen)₂(dppz)]²⁺ with CT-DNA²⁵ has also been included.

**Fig. 7** Entropy–enthalpy compensation plots constructed from the ITC derived binding data for compounds **1** and **2** and Λ - and Δ -[Ru(phen)₂(dppz)]²⁺. ◆ = compound **1**. Δ = compound **2** (first binding phase). × = compound **2** (second binding phase). ○ = Λ - and Δ -[Ru(phen)₂(dppz)]²⁺ interaction with CT-DNA only. On the basis of their thermodynamics profiles these interactions have been partitioned into two groups.

In his recent analysis of small molecule duplex DNA binding substrates using compensation plots, Chaires has shown that intercalators and groove binders have distinctive thermodynamic signatures.³¹ In contrast to intercalation, which is largely enthalpically driven,³² groove binding is predominantly entropically driven,³³ while binding by a mixed motif substrate, such as echinomycin,³⁴ produces a signature similar to groove binding.

As Fig. 7 reveals, all the binding data for **1**, **2**, and [Ru(phen)₂(dppz)]²⁺ fall into two groups. The group towards

the upper left of the plot includes interactions dominated by large favorable entropic contributions with much smaller favorable, or even unfavorable, enthalpic contributions. This group is largely composed of interactions involving **2**, and the $[\text{Ru}(\text{phen})_2(\text{dppz})]^{2+}$ cations, although it also contains the interaction of **1** with Poly(dA).poly(dT). For the other, a much tighter cluster to the right of the first group, entropy changes are much smaller and so enthalpic contributions to free energy are proportionally higher. This group contains all the other interactions involving compound **1** and the single-phase binding of Poly(dA).poly(dT) by compound **2**. Using Chaires' criteria, it is therefore tempting to conclude that the first group involves groove-binding interactions, while the second involves intercalation; however, in this case, such an analysis is slightly simplistic.

It is well established that thermodynamic profiles for interactions with Poly(dA).poly(dT) are often anomalous:³⁵ studies involving many intercalators,³⁶ groove-binders,³⁷ and DNA binding protein motifs³⁸ show that binding to this sequence is strongly entropically driven, even when favorable enthalpy contributions dominate the same molecules interaction with other sequences. In this context, the entropically driven binding of Poly(dA).poly(dT) by the "pure intercalator" **1** is not unusual. It has been suggested that this distinctive thermodynamic signature is the result of extensive binding induced solvent release as the minor groove "spine of hydration" involving highly ordered water molecules is disrupted.³⁹

In this context, the thermodynamic signature for the interaction between **2** and Poly(dA).poly(dT), which it is both entropically and enthalpically, driven is more unusual. However, similar thermodynamic profiles have been reported for a few other small molecules that bind to this polynucleotide. For example, studies on the minor groove binder berenil involving a variety of polynucleotides, show that high-affinity binding to Poly(dA).poly(dT) is driven by large favorable enthalpies and entropies.⁴⁰ Furthermore, binding to A-tracts by the intercalators ethidium bromide and particularly propidium iodide reveal thermodynamic signatures⁴¹ that are very similar to that displayed by **2**.

Conclusions

Modulating *in cellulo* DNA function can be achieved by developing novel nucleic acid binding agents capable of sequence and structure specific recognition. Small organic and metallo-intercalators potentially have a key role towards this end. In this paper we have used the basic dipyrrophenazine ligand and functionalized it with spermine-like amine chain in an extension to our earlier synthesis and characterization of the bipyridylium dppz derivatives. We have found that binding to DNA is greatly affected by the location of these chains on the dppz intercalative platform: if two chains are appended to the 3 and 6 positions of the basic dppz framework, very weak binding to DNA is observed, whereas a single chain attached to the end of the phenazine unit results in a system with good water solubility that binds to DNA with high affinities. Since dppz itself is water insoluble it cannot bind to DNA and thus structural data on this system is lacking. However, some evidence for the contrasting binding properties of **2** and **3** may be gathered from recent structural studies that revealed that compound **1** binds "side-on" into the major groove of DNA, parallel to base-pair steps.⁴² While it would be possible

for compound **2** to take up a similar alignment with the appended alkyl chain aligned within a groove, compound **3** cannot take up this position as one of the chains will clash with the floor of the groove.

Biophysical analysis on compound **2** confirms that it binds through intercalation. Whilst UV and luminescence titration data indicate that binding is modest ($\sim 10^5 \text{ M}^{-1}$) more detailed thermodynamic analysis using ITC indicate that for CT-DNA there is actually two types of binding site, one tight and one weaker with both binding events being entropically driven. The interaction of compound **2** with three synthetic polynucleotides also revealed biphasic binding, with both high-affinity and lower affinity binding sites being enthalpically and entropically driven, however in this case affinities up to the nanomolar range are observed. In contrast, Poly(dA).poly(dT) exhibits just one type of lower affinity binding site. An analysis of the data shows that compound **2** is capable of binding to oligonucleotides with higher affinities and selectivity than the previously reported bipyridylium derivative, **1**, and dppz metal complexes such as $[\text{Ru}(\text{phen})_2(\text{dppz})]^{2+}$

This study demonstrates that attachment of water-soluble spermine-like amine chains to an intercalating moiety can increase binding free energy by several orders of magnitude in comparison to the intercalator moiety on its own. The increase in binding free energy arises mainly through favorable interactions of the amine side-chain with the DNA grooves where it forms favorable hydrophobic interactions and probably removes site-specific water molecules in an entropically favorable process. Although it is clear that the compound selects for flexible sequences, future NMR and binding studies will focus on a detailed structural insight into binding at these sites. Such studies will also be aimed at providing further information into the biphasic nature of binding to most sequences.

Additionally, given the potent photo-oxidant properties of the parent dppz molecule, the photochemistry of free and DNA-bound compound **2**, and related analogues, will be further investigated. Such work exploring the potential of these organic systems to act as DNA sequence, structure and property analogous to previously reported metal ion-based redox probes¹ will form the basis of future reports. Their potential as possible therapeutics in live cells will also be explored.

Materials. Commercially available materials were used as received. Dipyrrophenazine-11-carboxylic acid and dipyrrophenazine-3,6-dicarboxylic acid were synthesized using adapted literature procedures. All reactions were carried out under an inert argon atmosphere. Calf thymus DNA (CT-DNA) was purchased from Sigma chemical company. It was purified by phenol extraction until Abs 260 nm/Abs 280 nm was >1.9 . Poly(dA).poly(dT), poly(dA-dT).poly(dA-dT), poly(dG).poly(dC) and poly(dG-dC).poly(dG-dC) were purchased from Amersham Pharmacia Biotech. Each sample was dissolved in 2 mL of 5 mM Tris, 25 mM NaCl buffer and dialyzed as per CT-DNA. Absorption and luminescence titrations were carried out in 25 mM NaCl, 5 mM TRIS pH7.0 buffer made with doubly distilled water (Millipore). The concentration of the DNA was determined *via* UV-Visible spectroscopy using the following extinction coefficients: CT-DNA $\epsilon_{260} = 6600 \text{ M}^{-1} \text{ cm}^{-1}$ for CT-DNA, $\epsilon_{260} = 12000 \text{ M}^{-1} \text{ cm}^{-1}$ for poly(dA).poly(dT),

$\epsilon_{262} = 13200 \text{ M}^{-1} \text{ cm}^{-1}$ for poly(dA-dT):poly(dA-dT), $\epsilon_{253} = 14800 \text{ M}^{-1} \text{ cm}^{-1}$ for poly(dG):poly(dC), $\epsilon_{254} = 16800 \text{ M}^{-1} \text{ cm}^{-1}$ for poly(dG-dC):poly(dG-dC) visible spectrophotometer. Emission spectra were recorded on a Hitachi F4500 spectrophotometer. The melting points (T_m) of double stranded DNA were carried out using a 1 cm path length Teflon stoppered quartz cuvette. Relative changes in absorbance at 260 nm were used to follow the melting point. Samples were prepared in 5 mM Tris, 25 mM NaCl buffer, using typical concentrations of 50 μM of DNA and 4–12 μM of compound. The temperature ramp was initiated around 35 °C and increased at a rate of 0.25 °C per minute until 99 °C. The temperature was monitored directly using a probe in an adjacent cuvette, the slow rate allows the solutions to reach the required temperature, without any lag. Viscosity experiments were carried out on a Cannon–Manning semi-micro viscometer (size 50) immersed in a thermostated water bath maintained at 27 ± 1 °C. The concentration of CT-DNA was kept between 0.5–1 mM bp⁻¹, and approximately 200 bp in length, to minimize complexities arising from DNA flexibility. The different samples were prepared by adding ligand to the DNA solution to give an increase in the ligand/bp ratio (solutions were made up so that values of 1/R (R = [DNA]/[ligand]) were between 0 and 0.2). The flow times (time taken for the solution to pass through the capillary tube) were recorded in triplicate and the average calculated after thermal equilibration of 20 min. ITC experiments were conducted using a VP-ITC from MicroCal LLC (Northampton MA, USA) interfaced to a Gateway PIII PC. Data acquisition and analysis was performed using Origin 5.0 (MicroCal LLC) and all titrations were performed at 25 °C in the 5 mM Tris, 25 mM NaCl, pH 7.0. The reference cell was filled with distilled water. The sample cell was filled with DNA (typical concentration of around 0.1–0.3 mM) and approximately 290 μL of the ligand (concentration between 0.5–1.5 mM) was loaded into the syringe and titrated into the DNA solution. After an initial injection of 3 μL , 18 injections of 15 μL each performed with a separation of 300–800 s depending on the rate with which the experiment returned to the baseline. The DNA solution was stirred continuously at 300 rpm throughout the experiments, which were maintained at 25 °C. Heats of dilution for each compound were determined by titrating the complex into the buffer solution. These dilution heats were subtracted from the ΔH° value for DNA-complex titration to give a corrected heat effect. Each titration was repeated at least two times and the average of ΔH° was calculated.

Acknowledgements

IH thanks the Foulkes Foundation for a fellowship during this research. We are grateful to EPSRC for providing a studentship for TP

Notes and references

- 1 J. E. Dickenson and L. A. Summers, *Aust. J. Chem.*, 1970, **23**, 1023.
- 2 (a) K. E. Erkkila, D. T. Odom and J. K. Barton, *Chem. Rev.*, 1999, **99**, 2777; (b) C. Metcalfe and J. A. Thomas, *Chem. Soc. Rev.*, 2003, **32**, 215; (c) B. M. Zeglis, V. C. Pierre and J. K. Barton, *Chem. Commun.*, 2007, 4565; (d) V. W.-W. Yam, K. K.-W. Lo, K.-K. Cheung and R. Y.-C. Kong, *J. Chem. Soc., Chem. Commun.*, 1995, 1191.
- 3 (a) A. E. Friedman, J. C. Chambron, J. P. Sauvage, N. J. Turro and J. K. Barton, *J. Am. Chem. Soc.*, 1990, **112**, 4960; (b) E. J. C. Olson, D. Hu, A. Hörmann, A. M. Jonkman, M. R. Arkin, E. D. A. Stemp, J. K. Barton and P. F. Barbara, *J. Am. Chem. Soc.*, 1997, **119**, 11458; (c) B. Önfelt, P. Lincoln, B. Nordén, J. S. Baskin and A. H. Zewail, *Proc. Natl. Acad. Sci. U. S. A.*, 2000, **97**, 5708.
- 4 See for example: B. Elias, C. Creely, G. W. Doorley, M. M. Feeney, C. Moucheron, A. Kirsch-De Mesmaeker, J. Dyer, D. C. Grills, M. W. George, P. Matousek, A. W. Parker, M. Towrie and J. M. Kelly, *Chem. Eur. J.*, 2008, **14**, 369 and references therein.
- 5 (a) B. Elias and A. Kirsch-De Mesmaeker, *Coord. Chem. Rev.*, 2006, **250**, 1627; (b) O. Van Gijte and A. Kirsch-De Mesmaeker, *J. Chem. Soc., Dalton Trans.*, 1999, 951; (c) L. Ghizdavu, F. Pierard, S. Rickling, S. Aury, M. Surin, D. Beljonne, R. Lazzaroni, P. Murat, E. Defrancq, C. Moucheron and A. Kirsch-De Mesmaeker, *Inorg. Chem.*, 2009, **48**, 10988.
- 6 (a) C. Metcalfe, M. Webb and J. A. Thomas, *Chem. Commun.*, 2002, 2026; (b) C. Metcalfe, H. Adams, I. Haq and J. A. Thomas, *Chem. Commun.*, 2003, 1152; (c) C. Metcalfe, I. Haq and J. A. Thomas, *Inorg. Chem.*, 2004, **43**, 317; (d) C. Metcalfe, C. Rajput and J. A. Thomas, *J. Inorg. Biochem.*, 2006, **100**, 1314; (e) C. Rajput, R. Rutkaite, L. Swanson, I. Haq and J. A. Thomas, *Chem. Eur. J.*, 2006, **12**, 4611; (f) S. P. Foxon, M. Towrie, A. W. Parker, M. Webb and J. A. Thomas, *Angew. Chem., Int. Ed.*, 2007, **46**, 3686; (g) M. R. Gill, J. Garcia-Lara, S. J. Forster, C. Smythe, G. Battaglia and J. A. Thomas, *Nat. Chem.*, 2009, **1**, 662.
- 7 (a) T. Phillips, I. Haq, A. J. H. Meijer, H. Adams, I. Soutar, L. Swanson, M. J. Sykes and J. A. Thomas, *Biochemistry*, 2004, **43**, 13657; (b) T. Phillips, C. Rajput, L. Twyman, I. Haq and Jim A. Thomas, *Chem. Commun.*, 2005, 4327.
- 8 D. A. McGovern, A. Selmi, J. E. O'Brien, J. M. Kelly and C. Long, *Chem. Commun.*, 2005, 1402.
- 9 (a) M. Yuki, V. Grukhin, C.-S. Lee and I. S. Haworth, *Arch. Biochem. Biophys.*, 1996, **325**, 39; (b) S. Lindemose, P. E. Nielsen and N. E. Møllegaard, *Nucleic Acids Res.*, 2005, **33**, 1709.
- 10 (a) N. Schmid and J. P. Behr, *Biochemistry*, 1991, **30**, 4357; (b) H. Deng, V. A. Bloomfield, J. M. Benevides and G. J. Thomas Jr, *Nucleic Acids Res.*, 2000, **28**, 3379.
- 11 (a) C. V. Kumar and E. H. Asuncion, *J. Am. Chem. Soc.*, 1993, **115**, 8547; (b) N. K. Modukuru, K. J. Snow, B. S. Perrin Jr., J. Thota and C. V. Kumar, *J. Phys. Chem. B*, 2005, **109**, 11810; (c) M. R. Duff, W. B. Tan, A. Bhamhani, B. S. Perrin Jr., J. Thota, A. Rodger and C. V. Kumar, *J. Phys. Chem. B*, 2006, **110**, 20693.
- 12 (a) A. Rodger, I. S. Blagbrough, G. Adlam and M. L. Carpenter, *Biopolymers*, 1994, **34**, 1583; (b) I. S. Blagbrough, S. Taylor, M. L. Carpenter, V. Novoselskiy, T. Shamma and I. S. Haworth, *Chem. Commun.*, 1998, 929; (c) J.-G. Delcros, S. Tomasi, S. Carrington, B. Martin, J. Renault, I. S. Blagbrough and P. Uriac, *J. Med. Chem.*, 2002, **45**, 5098.
- 13 P. M. Cullis, L. Merson-Davies and R. Weaver, *J. Am. Chem. Soc.*, 1995, **117**, 8033.
- 14 L. Wang, H. L. Price, J. Juusola, M. Kline and O. I. Phanstiel, *J. Med. Chem.*, 2001, **44**, 3682.
- 15 D. Ossipov, E. Zamaratski and J. Chattopadhyaya, *Helv. Chim. Acta*, 1999, **82**, 2186.
- 16 (a) D. Ossipov, P. I. Pradeepkumar, M. Holmer and J. Chattopadhyaya, *J. Am. Chem. Soc.*, 2001, **123**, 3551; (b) D. Ossipov, S. Gohil and J. Chattopadhyaya, *J. Am. Chem. Soc.*, 2002, **124**, 13416.
- 17 A. M. S. Garas and R. S. Vagg, *J. Heterocycl. Chem.*, 2000, **37**, 151.
- 18 S. Far, A. Kossanyi, C. Verchère-Béaur, N. Gresh, E. Taillander and M. Perrée-Fauvet, *Eur. J. Org. Chem.*, 2004, 1781.
- 19 (a) H. D. Stoeffler, N. B. Thornton, S. L. Temkin and K. S. Schanze, *J. Am. Chem. Soc.*, 1995, **117**, 7119; (b) J. Dyer, W. J. Blau, C. G. Coates, C. M. Creely, J. D. Gavey, M. W. George, D. C. Grills, S. Hudson, J. M. Kelly, P. Matousek, J. J. McGarvey, J. McMaster, A. W. Parker, M. Towrie and J. A. Weinstein, *Photochem. Photobiol. Sci.*, 2003, **2**, 542.
- 20 See for example C. V. Kumar, J. K. Barton and N. J. Turro, *J. Am. Chem. Soc.*, 1985, **107**, 5518.
- 21 J. D. McGhee and P. H. von Hippel, *J. Mol. Biol.*, 1974, **86**, 469.
- 22 (a) S. Satyanarayana, J. C. Dabrowiak and J. B. Chaires, *Biochemistry*, 1992, **31**, 9319; (b) S. Satyanarayana, J. C. Dabrowiak and J. B. Chaires, *Biochemistry*, 1992, **32**, 2573.
- 23 (a) F. G. Looontiens, P. Regenfuss, A. Zechel, L. Dumortier and R. M. Clegg, *Biochemistry*, 1990, **29**, 9029; (b) I. Haq, J. E. Ladbury, B. Z.

- Chowdhry, T. C. Jenkins and J. B. Chaires, *J. Mol. Biol.*, 1997, **271**, 244.
- 24 (a) I. Haq, T. C. Jenkins, B. Z. Chowdhry, J. Ren and J. B. Chaires, *Methods Enzymol.*, 2000, **323**, 373; (b) I. Haq, T. C. Jenkins and B. Z. Chowdhry, *Methods Enzymol.*, 2000, **340**, 109.
- 25 I. Haq, P. Lincoln, D. Suh, B. Nordén, B. Z. Chowdhry and J. B. Chaires, *J. Am. Chem. Soc.*, 1994, **117**, 4788.
- 26 H. P. Hopkins, J. Fumero and W. D. Wilson, *Biopolymers*, 1990, **29**, 445.
- 27 (a) H. C. M. Nelson, J. T. Finch, B. F. Luisi and A. Klug, *Nature*, 1987, **330**, 221; (b) T. E. Haran and U. Mohanty, *Q. Rev. Biophys.*, 2009, **42**, 41.
- 28 (a) M. McCall, T. Brown and O. Kennard, *J. Mol. Biol.*, 1985, **183**, 385; (b) M. H. Sarma, G. Gupta and R. H. Sarma, *Biochemistry*, 1986, **25**, 3659; (c) N. V. Hud and J. Plavec, *Biopolymers*, 2003, **69**, 144.
- 29 (a) M. J. Packer, M. P. Dauncey and C. A. Hunter, *J. Mol. Biol.*, 2000, **295**, 71; (b) E. J. Gardiner, C. A. Hunter, M. J. Packer, D. S. Palmer and P. Willett, *J. Mol. Biol.*, 2003, **332**, 1025.
- 30 (a) Y. Kim, J. H. Geiger, S. Hahn and P. B. Sigler, *Nature*, 1993, **365**, 512; (b) J. L. Kim, D. B. Nikolov and S. K. Burley, *Nature*, 1993, **365**, 520.
- 31 (a) J. B. Chaires, *Arch. Biochem. Biophys.*, 2006, **453**, 26; (b) J. B. Chaires, *Annu. Rev. Biophys.*, 2008, **37**, 135.
- 32 J. Ren, T. C. Jenkins and Jonathan B. Chaires, *Biochemistry*, 2000, **39**, 8439.
- 33 S. Mazur, F. A. Tanius, D. Ding, A. Kumar, D. W. Boykin, I. J. Simpson, S. Neidle and W. D. Wilson, *J. Mol. Biol.*, 2000, **300**, 321.
- 34 F. Leng, J. B. Chaires and Michael J. Waring, *Nucleic Acids Res.*, 2003, **31**, 6191.
- 35 K. J. Breslauer, D. P. Remeta, W.-Y. Chou, R. Ferrante, J. Curry, D. Zaunczkowski, J. G. Snyder and L. A. Markey, *Proc. Natl. Acad. Sci. U. S. A.*, 1987, **84**, 8922.
- 36 (a) D. P. Remeta, C. P. Mudd, R. L. Berger and K. J. Breslauer, *Biochemistry*, 1991, **30**, 9799; (b) J. Ren and J. B. Chaires, *Biochemistry*, 1999, **38**, 16067.
- 37 (a) L. A. Markey and K. J. Breslauer, *Proc. Natl. Acad. Sci. U. S. A.*, 1987, **84**, 4359; (b) J. Lah and G. Vesnaver, *J. Mol. Biol.*, 2004, **342**, 73.
- 38 T Cui, S. Wei, K. Brew and F. Leng, *J. Mol. Biol.*, 2005, **325**, 629.
- 39 X. Shui, L. McFail-Isom, G. G. Hu and L. D. Williams, *Biochemistry*, 1998, **37**, 8341.
- 40 (a) H.-U. Schmitz and W. Hübner, *Biophys. Chem.*, 1993, **48**, 61; (b) D. S. Pilch, M. A. Kirolos, X. Liu, G. E. Plum and K. J. Breslauer, *Biochemistry*, 1995, **34**, 9962.
- 41 (a) L. A. Markey and R. B. Macgregor Jr, *Biochemistry*, 1995, **34**, 9962; (b) F. Han and T. V. Chalikian, *J. Am. Chem. Soc.*, 2003, **125**, 7219.
- 42 P. Waywell, J. A. Thomas and M. P. Williamson, *Org. Biomol. Chem.*, 2010, **8**, 648.